Study of the Structural and Thermal Properties of Aluminum-Copper-Zinc Alloys

Raiq Rafi Omar Al-Nima[1, a)] and Mahmood Ahmad Hamood[1, b)]

[1]*Department of Physics, College of Science, University of Mosul, Mosul, Iraq*

[a)] *Corresponding author: raiq.scp83@student.uomosul.edu.iq*
[b)] *dr.mahmood@uomosul.edu.iq*

Abstract. Phase Change Materials (PCMs) are gaining increasing importance in energy storage systems due to their high energy storage densities. These materials store energy by exploiting the latent heat of fusion or vaporization during phase transitions. Optimizing the crystal structure and microstructure of these materials enhances their thermal stability. This paper addresses an important thermodynamic aspect, namely the Specific Heat Capacity (SHC), of aluminum alloys widely used in industry. Various applications (from heat treatment to corrosive materials) demonstrate that SHC (as an intensive property) or SHC (as an extended property) is a fundamental concept in thermodynamics and of great importance in practical applications. In this research, a set of ternary alloys, $Al_{90}Cu_{10-x}Zn_x$, with different elemental concentrations Zn (x=0, 2, 4, 6, 8, 10), are fabricated by pouring the molten material into specially designed molds. The structural and thermal properties of the samples are studied and it is found that these properties are affected by the partial replacement of Copper with Zinc.

Keywords: Specific Heat Capacity, Ternary Alloys, Aluminum, Copper, Zinc

INTRODUCTION

Cast alloys are employed in many wide range fields such as transportation, electricity, packaging, devices, tools, machines and aircrafts industry [1][2]. Knowledge and preparation of elements are essential steps in manufacturing alloys. The prepared elements are combined together, they can be two or more elements of different mixing ratios. The combined elements are melted in a furnace under a high temperature. So, the produced alloys will have new characteristics of thermal, optical, electrical, ... etc. The elements can be Aluminum (Al), Copper (Cu), Tin (Sn), Zinc (Zn), Magnesium (Mg), Manganese (Mn), Silicon (Si), iron (Fe) and others [3][4][5].Then, manufactured alloys are subjected to several mechanical tests such as hardness, compression, fatigue resistance, sheer stress, SHC and XRD [6][7][8]. Al and Cu-based casting alloys are widely used worldwide in high-strength industrial applications due to their low density and ability to be cast into complex shapes. Currently, these alloys are widely used in the manufacture of engine components, including blocks, cylinder heads, pistons, intake manifolds, and brackets, where they have replaced cast iron components in many cases [9-11]. Recently, the Al-Cu alloys system has received considerable attention due to its outstanding hardening properties and excellent performance at high temperatures, which are often the weak point of conventional aluminum alloys [12, 13]. Furthermore, small amounts of other alloying elements, such as Zn, significantly improve the thermal properties of the alloys produced. This is due to the formation of precipitates of alloying phases with aluminum, which form during heat treatment and inhibit dislocation movements [14-16]. Zn is the key element for developing the strength and hardness of heat-treated Al-Cu alloys. In heat-treated conditions, the CuZn solidification stage has a melting point equal to the melting point, beyond which no further strengthening or softening of the matrix occurs [17, 18]. At room temperature, scientific research has identified the quantities of Zn that can be added to an Al-Cu alloy to achieve the best of thermal properties Zn also has a beneficial effect on SHC. The main contributions of this paper are:

- Manufacturing cast Al, Cu, and Zn alloys from pure elements with varying weight ratios.
- Applying different thermal property evaluations to manufactured cast alloys, based on SHC.
- Performing compositional measurements of manufactured samples, such as XRD.
- Conducting comprehensive comparisons of results between manufactured cast alloys.

This research aims to utilize the studied cast alloys in vital industries, such as aircraft and ship heat engines.

PROPOSED METHOD

Alloys can be prepared in several stages. The first stage involves obtaining the physical elements Al, Cu, and Zn. The second stage involves preparing pure Al, Cu, and Zn castings. The third stage involves applying variable weight percentages during the manufacture of the castings. The fourth stage involves cutting the castings into uniform pieces. The fifth stage involves grinding each casting, taking into account multiple measurements of the cutting ratio (R). The sixth stage involves considering compositional and thermal tests for SHC and XRD for evaluation. The final stage involves analyzing, comparing, and measuring the recorded results. Figure 1. illustrates the main schematic diagram of the extensive processes involved in this study.

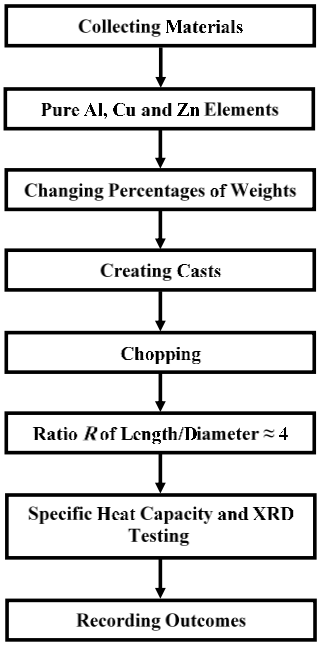

FIGURE 1. The main block diagram of the extensive processes in this study

Cu was melted at high temperatures in an electric furnace, and Al was subsequently incorporated and combined with Cu in the electric furnace. Zn was then incorporated and combined with Cu-Al in the electric furnace once again. Table 1 shown concentration of the elements.

TABLE 1. The used ratios and weights for the Al, Cu and Zn

Index	Al(gm)	Cu(gm)	Zn(gm)	Al (%)	Cu (%)	Zn (%)
A1	18	2	0	90	10	0
A2	18	1.6	0.4	90	8	2
A3	18	1.2	0.8	90	6	4
A4	18	0.8	1.2	90	4	6
A5	18	0.4	1.6	90	2	8
A6	18	0	2	90	0	10

The prepared elements were then carefully melted and mixed together until homogeneous, finally forming an Al-Cu-Zn casting. These processes were repeated several times to obtain different Al-Cu-Zn cast alloys. The cutting characteristics of the obtained cast alloys are then considered. Each cast alloy was machined using the cutting ratio (R), where R is defined as the length per diameter. In this study, the cutting ratio is taken as R ≈ 4 measurements of testing SHC and XRD. 6 pieces are cut evenly with regular measurements. Finally, some thermal and structural properties are tested.

SHC of the material in any temperature depends on the thermal conductivity of material; it is a fundamental concept of thermodynamics. It can have a fixed volume according to its components, which are represented by:

$$C_v = C_l + C_e + C_M + C_o \tag{1}$$

where: C_v is the SHC at volume constant, C_l is the SHC of phonons, C_e is the SHC of conduction electrons, C_M is the SHC related to the excitation of magnetic moments (magnon) and C_o is the component of the SHC connected with the creation of vacancies, order-disorder transition, … etc. [19].

Heat capacity is an extensive property, whilst, SHC is an intensive property. It is defined as the heat amount that is required to raise the temperature of one substance gram by one Celsius. The unit is joule per kelvin. Heat capacity equals to mass of material multiplied by specific heat [20].

SHC is divided into two parts: SHC at pressure constant (C_p) and SHC at volume constant (C_V). It can be expressed as:

$$\left(\frac{\partial H}{\partial T}\right)_P = \left(\frac{\partial Q}{\partial T}\right)_P = C_P \quad (2)$$

$$\left(\frac{\partial U}{\partial T}\right)_V = \left(\frac{\partial Q}{\partial T}\right)_V = C_V \quad (3)$$

where: $\left(\frac{\partial H}{\partial T}\right)_P$ is the enthalpy of the system and $\left(\frac{\partial U}{\partial T}\right)_V$ is the internal energy of a closed system [20].

Specific heat capacities of Al, Cu, Zn and Sn equal to 0.897 J/(g. K), 0.385 J/(g. K), 0.387 J/(g. K), 0.227 J/(g. K) and 1.012 J/(g. K) [21].

Testing SHC is utilized for R≈4. A total of 6 pieces of cast alloys are manufactured for Al-Cu-Zn. Each sample is computed for: the amount of acquired heat (Q_{Acq}) of Water & Calorimeter ($W\&C$), and the amount of lost heat (Q_{lost}) of alloy ($Alloy$). All samples have temperature calculations before being inside the electric furnace, and then, after few minutes of being inside the electric furnace. More calculations are also considered for $W\&C$. Such processes of putting the samples inside the electric furnace and taking them out are utilized for the computation of temperature differences between the amount of acquired heat and the amount of lost heat. See the following equation:

$$[Q_{lost}]_{Alloy} = [Q_{Acq}]_{W\&C} \quad (4)$$

Hence, the SHC of alloy is calculated as a measured $[C_p]_{Alloy}$, which can be expressed as follows:

$$[C_p]_{Alloy} = \frac{\left[\left(mC_{p_W} + mC_{p_C}\right)\times(T_f - T_i)\right]_{W\&C}}{[m_{Alloy}\times(T_F - T_f)]_{Alloy}} \quad (5)$$

where: $[C_p]_{Alloy}$ is the SHC of alloy, C_{p_W} is the SHC of Water, $C_{p_{Cu}}$ is the SHC of calorimeter, m_{Alloy} is the mass of alloy, m_{Water} is the mass of water, m_{cu} is the mass of copper, T_f is the final temperature, T_i is the initial temperature and T_F is the furnace temperature [20]. Employed measurements' outcomes for the established cast alloys are recorded and compared.

It is worth mentioning that the error margins of the SHC computations can be related to adding water to the cast alloys. To illustrate, if the cast alloy is partially covered by water, this causes problems in SHC computations. This is reasonable because only part of the cast alloy would affect for SHC.

RESULTS AND DISCUSSION

The SHC and XRD of Al-Cu-Zn ternary alloys is tested. First, the mass of the calorimeter, water, and each sample is calculated. Second, the specific heat values of the calorimeter and water are obtained. Finally, the SHC of each cast alloy is calculated. There are some important points to highlight here. The SHC of the alloys is calculated from Equations (4) and (5). They are explained as follows:

1- The mass of the calorimeter when empty (m_Cu) is taken into account.

2- The mass of the water and the amount of the calorimeter in water are calculated. The mass of the calorimeter when empty is then subtracted to find the mass of water (m_W).

3- The mass of each sample (m_ Alloy) is also taken into account.

4- The initial temperature of the water is measured before the sample is placed in the electric furnace (T_i). The sample is placed inside the electric furnace at a low temperature for a few minutes. The final temperature of the water is calculated after the sample is removed from the electric furnace and placed in the water (T_f). With further illustrations, each sample is removed from the electric furnace and then immersed in water. The final temperature is then measured after thermal equilibration between the calorimeter, the water, and the sample. The amount of heat lost to any cast alloy is equal to the amount of heat gained from the $W\&C$.

Detailed analysis of SHC trends with incremental Zn additions is given Table 2, it provides useful insights into material optimization for industrial applications. So, this table has details of the SHC measurements for cast Zn alloys. The SHC test for Al-Cu-Zn ternary alloys is considered.

TABLE 2. Relationships between the employed elements ratios and SHC for the Zn

Index	Zn (wt%)	Zn (gm)	Cp of Alloy (J/g. k) for Zn
A1	0	0	0.101809521
A2	2	0.4	0.115332015
A3	4	0.8	0.123600088
A4	6	1.2	0.067108596
A5	8	1.6	0.075403471
A6	10	2	0.092304823

From this table, it can be seen that the Zn has been incrementally increased. As mentioned, this provides useful insights into material optimization. That is, this leads to slightly fluctuated effects to the SHC. It is incrementally increased when Zn weight percentages increased. Then, it is decreased when Zn weight percentage equals to 6wt%. Subsequently, it is increased again while Zn weight percentage keeps increasing. The manufacture of a set of Al-Cu-Zn alloys. The study also investigated the effect of Zn addition, taking into account the thermal properties of the manufactured alloys. The manufacture of cast alloys using these elements is expected to be of great exploration value, as the cast alloys are expected to acquire new properties [22]. One of the most important properties of cast materials is that when an alloying element is added to the main matrix, different primary and secondary phases of the alloying elements are formed. These phases have a significant impact on the crystal structure, altering the alloy's properties, efficiency, and performance. Therefore, one of the thermal properties that changes is the melting point [23]. Consequently, the melting point varies, either increasing or decreasing, depending on the concentration of the alloying element. This is confirmed by the equilibrium diagram for any alloy [24].

This increase or decrease in melting point is the result of intermolecular forces. One of the most important factors affecting the melting point of a material is the type of forces that bind the molecules it contains. The stronger the intermolecular bonds, the higher their melting points, which significantly affects the energy stored in the alloy, which in turn affects its SHC [25]. Therefore, the specific heat kinetics of the resulting alloys are shown in Figure 2. We find that the SHC of Al, Cu, and Zn alloys increases until the Zn concentration reaches 4%, indicating an increase in the alloy's melting point. The SHC then begins to decrease beyond this concentration until it reaches 6%, after which the SHC begins to rise again.

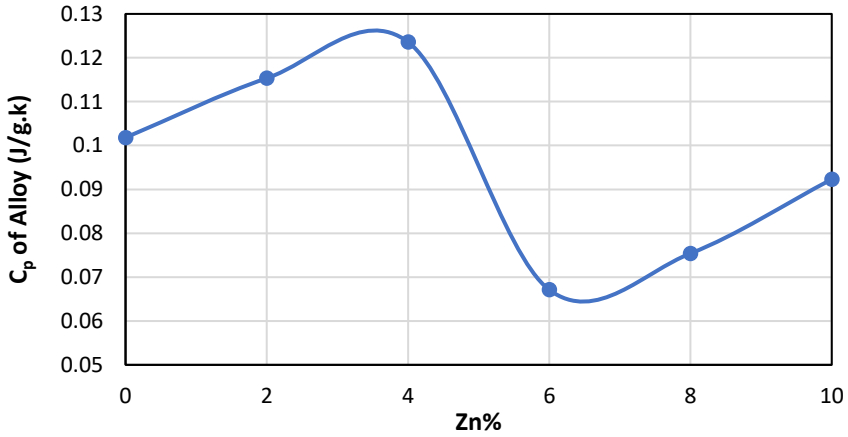

FIGURE 2. Relationships between the ratios of elements' weights and SHC for $Al_{90}Cu_{10-x}Zn_x$, x= (0, 2, 4, 6, 8, 10) %

XRD is used to test the phase states and crystal structures of the cast alloys, as shown in Figure 3. Charts provide XRD data for the Al-Cu-Zn cast alloys used. All figures show the Al-Cu-Zn cast alloys and the phase decomposition confirmed by XRD tests. Four phases are detected in each tested cast alloy: Al_2Cu, $Al_{0.4}Zn_{0.6}$, Al_4Cu_9, and CuZn. In all tested cast alloys, the predominant phase is Al_2Cu, followed by Al_4Cu_9 as the second predominant phase [25]. $Al_{0.4}Zn_{0.6}$ is recorded as the third predominant phase. CuZn is reported as the least abundant phase [26]. Figure 3 and Table 3 afford the XRD tests for the utilized samples of Al-Cu-Zn cast alloy, the phases of the cast alloys used are analyzed using X'Pert HighScore Plus software, where XRD patterns are explored, peaks are obtained, and graphs

are compared. Each peak refers to a phase. So, the quantitive peaks that lead to obtained phases are determined as given in Table 3, where position [°2Th.], height [cts], hkl and phases are all valued in each peak. This would enhance more clarity in demonstrating. Full details of locations and values, especially for phases, can be verified. These tests are provided and successfully executed, and the results obtained are verified to be consistent with relevant tests.

TABLE 3. Analyzed XRD values for samples of Al-Cu-Zn cast alloys

1st Cast Alloy, $Al_{90}Cu_{10-x}Zn_x$, weight for x =0%				
No.	**Pos. [°2Th.]**	**Height [cts]**	**hkl**	**Phases**
1	39.09282	1231.44	111	Al_4Cu_9, Al
2	39.29239	1438.294	111	Al_4Cu_9, Al
3	45.41193	2002.196	020	Al
4	45.52102	1870.385	020	Al
5	65.83783	636.8271	330	Al
6	78.90259	1429.934	004	Al_2Cu, Al
2nd Cast Alloy, $Al_{90}Cu_{10-x}Zn_x$, weight for x =2%				
No.	**Pos. [°2Th.]**	**Height [cts]**	**hkl**	**Phases**
1	39.16205	2514.466	111 ،121	Al_4Cu_9, Al
2	39.27609	1805.628	111 ،121	Al_4Cu_9, Al
3	45.59215	2946.708	020 ،022	Al, $Al_{0.4}Zn_{0.6}$
4	45.71834	1271.772	020 ،022	Al, $Al_{0.4}Zn_{0.6}$
5	65.74242	917.597	022 ،040	Al, $Al_{0.4}Zn_{0.6}$
6	78.89973	1574.034	131 ،233	Al_2Cu, CuZn
3rd Cast Alloy, $Al_{90}Cu_{10-x}Zn_x$, weight for x =4%				
No.	**Pos. [°2Th.]**	**Height [cts]**	**hkl**	**Phases**
1	38.94427	1237.916	111	Al_4Cu_9, Al
2	44.93027	17112.82	020	Al, $Al_{0.4}Zn_{0.6}$
3	45.05595	24639.35	020	Al, $Al_{0.4}Zn_{0.6}$
4	45.11916	22831.46	020	Al, $Al_{0.4}Zn_{0.6}$
5	65.51379	2851.232	333,022	Al, $Al_{0.4}Zn_{0.6}$
6	78.67879	850.4598	131,004	Al_2Cu, CuZn
4th Cast Alloy, $Al_{90}Cu_{10-x}Zn_x$, weight for x =6%				
No.	**Pos. [°2Th.]**	**Height [cts]**	**hkl**	**Phases**
1	39.1525	1663.965	111	Al_4Cu_9, Al
2	39.26591	1350.376	111	Al_4Cu_9, Al
3	45.30387	4329.765	020	Al, $Al_{0.4}Zn_{0.6}$
4	45.46661	3460.329	020	Al, $Al_{0.4}Zn_{0.6}$
5	65.73527	617.1744	022	Al, $Al_{0.4}Zn_{0.6}$
6	78.7418	2034.916	131 ،121	Al_2Cu, CuZn
5th Cast Alloy, $Al_{90}Cu_{10-x}Zn_x$, weight for x =8%				
No.	**Pos. [°2Th.]**	**Height [cts]**	**hkl**	**Phases**
1	38.86736	2470.548	111	Al_4Cu_9, Al
2	38.98489	1794.481	111	Al_4Cu_9, Al
3	45.18999	1877.429	020	Al, $Al_{0.4}Zn_{0.6}$
4	45.30851	938.7147	020	Al, $Al_{0.4}Zn_{0.6}$
5	65.53804	1655.06	022	Al, $Al_{0.4}Zn_{0.6}$
6	78.63836	1268.556	131	Al_2Cu, CuZn
6th Cast Alloy, $Al_{90}Cu_{10-x}Zn_x$, weight for x =10%				
No.	**Pos. [°2Th.]**	**Height [cts]**	**hkl**	**Phases**
1	39.13487	2013.02	111	Al
2	39.30161	2146.524	111	Al
3	45.46102	2552.825	020	Al, $Al_{0.4}Zn_{0.6}$
4	65.91699	825.9559	022	Al, $Al_{0.4}Zn_{0.6}$
5	78.69502	769.9709	131	$Al_{0.4}Zn_{0.6}$
6	78.91686	1161.863	131	$Al_{0.4}Zn_{0.6}$

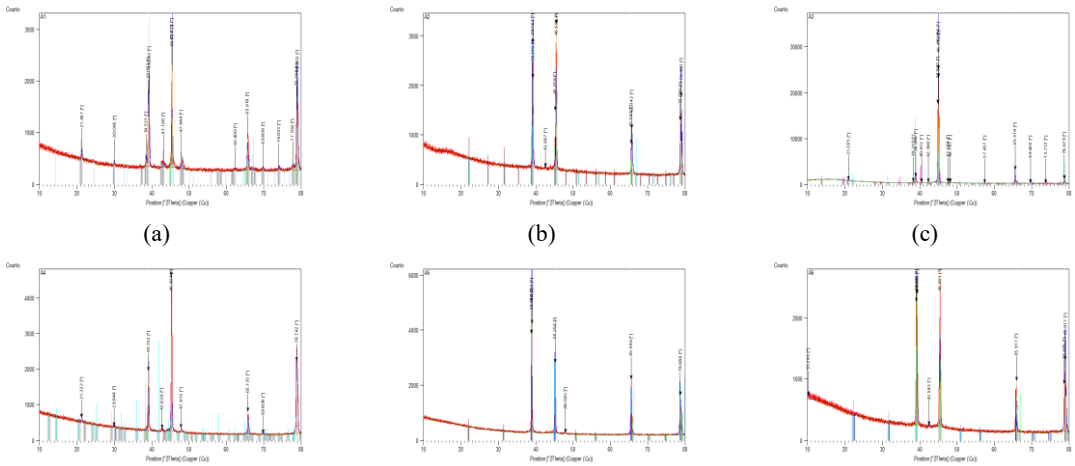

FIGURE 3. Appearances and analyses of XRD for samples of Al-Cu-Zn cast alloys which are considered with: $Al_{90}Cu_{10-x}Zn_x$ cast alloys (a) A1 for x =0%, (b) A2 for x =2%, (c) A3 for x =4%, (d) A4 for x =6%, (e) A5 for x =8%, and (f) A6 for x =10%

For interpreting Figure 3 in more depth, when conducting peak analysis for each diagram using the X'Pert HighScore program, the position of the atoms within the alloy is fixed. Miller indices are found to show the level and structure of the atoms. The main and secondary phases for each alloy are also identified. By studying the characteristics of each phase, a deep understanding and interpretation connected to SHC examinations can be found.

CONCLUSION

In this research paper, cast alloys of Aluminum, Copper, and Zinc elements are manufactured. The thermal and structural properties are studied. SHC of the alloys is also taken into account and it is found that the SHC fluctuates (increased and decreased) with the change in Zn concentration. The highest SHC value is recorded at the Zn concentration of 4% and the lowest value is reported at the concentration of 6%. The variation in these values could be explained as it is resulting from the amount of intermolecular forces or the bonding forces between molecules. The higher the bonding forces, the higher the melting point, the higher the SHC, and the higher the free energy or energy stored in the material. Similarly, the lower the bonding forces, the lower the melting point, the lower the SHC, and the lower the free energy or energy stored in the material. In addition to the above, the phases that appear through the interaction of the alloy elements in the liquid state at a certain temperature played a major role in all mechanical, physical and thermal properties.

As a clearer summary with specific recommendations for alloy industrial applications, practical implications of Al-Cu-Zn cast alloys for SHC can yield significantly improvements in various fields of industry, agriculture, and commerce. For industrial relevance, a further goal or aim can be represented by exploiting the considered cast alloys in critical industries such as building airplanes and ships.

ACKNOWLEDGEMENTS

First of all, many thanks to my supervisor (Prof. Dr. Mahmood A. A. Al-Juboori), the persons who positively supported me in the Ministry of Higher Education and Scientific Research in Iraq (MOHESR) and the Ministry of Education (ME), and all my valuable friends.

REFERENCES

1. R. R. O. Al-Nima and M. A. H. Al-jiboori, "Manufacturing Al-Cu-Mg Alloys and Studying Various Mechanical Properties," *Adv. Mech.*, **9**(3), pp. 291–311, (2021).
2. A. Ambroziak and M. T. Solarczyk, "Application and mechanical properties of aluminium alloys," in *Shell Structures: Theory and Applications*, **4**, CRC Press, (2017), pp. 525–528. doi: 10.1201/9781315166605.

3. R. Al-Nima and M. Al-jiboori, “Comprehensive Study for Impure and Pure Casts of Aluminum and Copper,” *Preprints*, (2021). doi: 10.20944/preprints202110.0040.v1.
4. R. R. Abdljabar and F. T. Saeed, “Synthesis and characterization of Mn (II), Co (II), Ni (II), Cu (II) and Zn (II) complexes with heterocyclic ligands and evaluation of its biological activity,” *Rafidain J. Sci.*, **33**(4), pp. 56–68, (2024), doi: 10.33899/rjs.2024.185384.
5. Y. A. Shekha and J. K. Mohammedamin, “Assessment of Heavy Metal Contamination in Dust Samples from Industrial and Non-Industrial Sites in Erbil Governorate,” *Rafidain J. Sci.*, **33**(3E), (2024), doi: 10.33899/rjs.2024.184537.
6. M. Sadawy, H. Metwally, H. Abd El-Aziz, A. Adbelkarim, H. Mashaal, and A. Kandil, “The role of Sn on microstructure, wear and corrosion properties of Al-5Zn-2.5 Mg-1.6 Cu-xSn alloy,” *Mater. Res. Express*, **9**(9), p. 96507, (2022), doi: 10.1088/2053-1591/ac8cd2.
7. F. N. M. Ali, R. Z. A. and Al- Fulayih, and Y. A. K. Salman, “Effect of Chromium Plating of AISI 321 Alloy at 1000 ° C on Fatigue Resistance Article information,” *Rafidain J. Sci.*, **33**(4), pp. 118–125, (2024), doi: 10.33899/rjs.2024.185389.
8. C. O. Ezenwelu, C. M. Okeke, O. I. Udemezue, O. R. Ngwu, J. Ogana, and E. H. Oparaji, “Assessment of Differential Sheer Stress Indices in Agricultural Soil Receiving Cafeteria Effluent,” *Rafidain J. Sci.*, **33**(1), pp. 42–48, (2024), doi: 10.33899/rjs.2024.182825.
9. K. Zheng, D. J. Politis, L. Wang, and J. Lin, “A review on forming techniques for manufacturing lightweight complex—shaped aluminium panel components,” *Int. J. Light. Mater. Manuf.*, **1**(2), pp. 55–80, (2018).
10. A. Banerjee, S. Raju, R. Divakar, and E. Mohandas, “High temperature heat capacity of alloy D9 using drop calorimetry based enthalpy increment measurements,” *Int. J. Thermophys.*, **28**(1), pp. 97–108, (2007), doi: 10.1007/s10765-006-0136-0.
11. E. A. Protopopov, S. S. Dobrykh, and A. A. Protopopov, “Estimation of Temperature Dependences of Specific Heat Capacity of Low-Alloy Steels,” *Int. J. Appl. Eng. Res.*, **13**(18), pp. 13536–13540, (2018).
12. I. L. Ferreira, J. A. de Castro, and A. Garcia, “Determination of heat capacity of pure metals, compounds and alloys by analytical and numerical methods,” *Thermochim. Acta*, **682**, pp. 1–7, (2019), doi: 10.1016/j.tca.2019.178418.
13. N. Zago, “Specific heat capacity evaluation of aluminium alloy powders via Fast Scanning Calorimetry,” MSc. Thesis, Dipartimento di Ingegneria Industriale DII Corso, UNIVERSITA’ DEGLI STUDI DI PADOVA, Italy, (2019).
14. F. J. Romero, M. C. Gallardo, J. M. Martín-Olalla, and J. del Cerro, “Experimental method to determine specific heat capacity and transition enthalpy at a first-order phase transition: Fundamentals and application to a Ni-Mn-In Heusler alloy,” *Thermochim. Acta*, **706**, (2021), doi: 10.1016/j.tca.2021.179053.
15. T. K. Akopyan, P. K. Shurkin, N. V Letyagin, F. O. Milovich, A. S. Fortuna, and A. N. Koshmin, “Structure and precipitation hardening response in a cast and wrought Al-Cu-Sn alloy,” *Mater. Lett.*, **300**, p. 130090, (2021), doi: 10.1016/j.matlet.2021.130090.
16. H. Xu, Y. Dong, S. Bai, and Z. Liu, “Effect of small Sn addition on the initial strengthening and microstructural evolution of an Al-Cu-Mg-Ag alloy,” *J. Alloys Compd.*, **943**, p. 169167, (2023), doi: 10.1016/j.jallcom.2023.169167.
17. P. Tan, Z. Liu, J. Qin, Q. Wei, B. Wang, and D. Yi, “Enhanced corrosion performance by controlling grain boundary precipitates in a novel crossover Al-Cu-Zn-Mg alloy by optimizing Zn content,” *Mater. Charact.*, **208**, p. 113615, (2024), doi: 10.1016/j.matchar.2023.113615.
18. R. R. O. Al-Nima, “Manufacturing Al-Cu and Al-Cu-Mg Alloys with Studying Some of their Mechanical Properties,” Master thesis, Department of Physics, University of Mosul, Iraq, (2021).
19. R. Przeliorz, M. Goral, G. Moskal, and L. Swadzba, “The relationship between specific heat capacity and oxidation resistance of TiAl alloys,” *J. Achiev. Mater. Manuf. Eng.*, **21**(1), pp. 47–50, (2007).
20. D. Dragulin and M. Rüther, “Specific heat capacity of aluminium and aluminium alloys,” *Prozesswarme*, **2018**(5), pp. 51–56, (2018).
21. S. H. Aleabi, A. W. Watan, E.M.-T. Salman, K. A. Jasim, A. H. Shaban, T. M. Alsaadi, The study effect of weight fraction on thermal and electrical conductivity for unsaturated polyester composite alone and hybrid, AIP Conference Proceedings, **1968**(1), 020019, (2018).
22. A. Villalta-Cerdas and C. McCleary, “Analysis of copper alloys as an introduction to data analysis and interpretation for General Chemistry courses,” *Educ. Química*, **30**(2), p. 41, (2019), doi: 10.22201/fq.18708404e.2019.2.67346.
23. M. A. A. Hasan, K. A. Jasim, , H. A. J. Miran, Korean Journal of Materials Research, **32**(2), pp. 66–71 (2022).
24. B. A. Omar, S. J. Fathi, K. A. Jassim, Effect of Zn on the structural and electrical properties of high

temperature HgBa2Ca2Cu3O8+δ superconductor, AIP Conference Proceedings, **1968**(1), 030047, (2018).
25. K. A. Jasim, The effect of cadmium substitution on the superconducting properties of Tl1-x Cd x Ba2Ca2Cu 3O9-δ compound, Journal of Superconductivity and Novel Magnetism, **26**(3), pp. 549–552, (2013).
26. N. S. Abed, S. J. Fathi, K. A. Jassim, S. H. Mahdi, Partial substitution of Zn Effects on the Structural and Electrical Properties of High Temperature Hg0.95Ag0.05Ba2Ca2Cu3O8+δ Superconductors, Journal of Physics: Conference Series, **1003**(1), 01209, (2018).